Металлофиз. новейшие технол. / Metallofiz. Noveishie Tekhnol.
2018, т. 40, № 10, сс. 1375–1385 / DOI: 10.15407/mfint.40.10.1375
Оттиски доступны непосредственно от издателя
Фотокопирование разрешено только
в соответствии с лицензией

PACS numbers: 61.05.cp, 61.43.Gt, 62.20.de, 62.20.Qp, 62.23.Pq, 81.20.Ev, 81.20.Wk

On the Advanced Mechanical Properties of Fe–Cu and Y–Cu Nanocomposites Obtained by Mechanical Alloying

M. Dashevskyi, N. Belyavina, O. Nakonechna, M. Melnichenko, and S. Revo

Taras Shevchenko National University of Kyiv,
Department of Physics,
R&D Laboratory of Metal and Ceramics Physics,
60 Volodymyrska Str.,
UA-01033 Kyiv, Ukraine

In this study, the Fe–Cu and Y–Cu nanocomposites are synthesized by mechanical alloying of the elemental powder mixture of the iron, copper and crushed yttrium particles in a high-energy planetary ball mill inside the argon atmosphere. Phase transformations in obtained composite materials are studied by X-ray powder-diffraction methods. The metastable supersaturated α-(Fe, Cu) solid solution is formed in the Fe–Cu nanocomposites during milling process, while the phase transformation during milling of the equiatomic Y–Cu mixture follows the reaction: $Y + Cu \rightarrow YCu + YCu_2$. All obtained materials demonstrate improved mechanical properties. A set of measurements of the mechanical characteristics is carried out. The hardness measured for both FeCu and YCu nanocomposites is higher than that for conventional bulk alloys due to the grains' refinement during milling process. Besides, the synthesized nanocomposites are characterized by relatively low values of the Young's modulus.

Key words: composite material, powder metallurgy, crystal structure, hardness, X-ray diffraction.

У роботі нанокомпозити Fe–Cu та Y–Cu було синтезовано шляхом механічного леґування порошкової суміші елементарних частинок заліза, міді та дробленого ітрію у високоенергетичному планетарному кульовому

Corresponding author: Sergiy Revo
E-mail: s_revo@i.ua

Citation: M. Dashevskyi, N. Belyavina, O. Nakonechna, M. Melnichenko, and S. Revo, On the Advanced Mechanical Properties of Fe–Cu and Y–Cu Nanocomposites Obtained by Mechanical Alloying, *Metallofiz. Noveishie Tekhnol.*, **40**, No. 10: 1375–1385 (2018), DOI: 10.15407/mfint.40.10.1375.

млині в атмосфері арґону. Фазові перетворення в одержаних композиційних матеріялах вивчали методами порошкової рентґенівської дифрактометрії. Встановлено, що під час розмелювання суміші порошків Fe та Cu в ній утворюється метастабільний пересичений твердий розчин α-(Fe, Cu), тоді як фазові перетворення в еквіатомовій суміші Y–Cu під час механохемічної активації відбуваються за реакцією $Y + Cu \rightarrow YCu + YCu_2$. Одержані матеріяли демонструють поліпшені механічні характеристики. Було виміряно відповідні механічні характеристики. Твердість обох нанокомпозитів FeCu та YCu є вищою, ніж у відповідних кристалічних стопів внаслідок зменшення розмірів зерен під час розмелювання. Крім того, синтезовані нанокомпозити характеризуються порівняно низькими значеннями модуля Юнґа.

Ключові слова: композиційний матеріял, порошкова металурґія, структура кристалів, твердість, рентґенівська дифрактометрія.

В работе нанокомпозиты Fe–Cu и Y–Cu были синтезированы путём механического легирования порошковой смеси элементарных частиц железа, меди и измельчённого иттрия в высокоэнергетической планетарной шаровой мельнице в атмосфере аргона. Фазовые превращения в полученных композиционных материалах были изучены методами порошковой рентгеновской дифрактометрии. Метастабильный пересыщенный твёрдый раствор α-(Fe, Cu) образуется в процессе размола в нанокомпозитах Fe–Cu, а при измельчении эквиатомной смеси Y–Cu происходит следующее фазовое превращение: $Y + Cu \rightarrow YCu + YCu_2$. Все полученные материалы имеют улучшенные механические свойства. Были измерены соответствующие механические характеристики. Твёрдость обоих нанокомпозитов FeCu и YCu выше, чем у обычных объёмных сплавов, из-за уменьшения размеров зёрен в процессе измельчения. Кроме того, синтезированные нанокомпозиты характеризуются относительно низкими значениями модуля Юнга.

Ключевые слова: композиционный материал, порошковая металлургия, кристаллическая структура, твёрдость, рентгеновская дифрактометрия.

(Received March 23, 2018)

1. INTRODUCTION

Intermetallic compounds and alloys often have excellent and attractive physical, chemical, electrical, magnetic and mechanical properties such as low density, high strength, high stiffness and nevertheless excellent corrosion resistance. Moreover, nanocrystalline metallic alloys in their metastable state (in particular, as a supersaturated solid solution) as well as the fine-grained intermetallic compounds are extremely attractive because of their functional potential [1]. A number of processing techniques have been developed to synthesize the nanocrystalline materials. Special attention should pay on mechanical alloying, which is the most promising and rapidly developing processing technique [2]. The

limits of solubility can also be enhanced significantly in mechanically alloyed systems even for immiscible elements [3, 4]. Repeated fracturing and welding of particles during mechanical alloying can result in appropriate mixing of constituents, which can lead to a change in solubility limits and formation of metastable solid solutions [2].

Nanocrystalline materials of the Fe–Cu system synthesized by mechanical alloying of elemental Fe and Cu powders have attracted close attention of researchers for a long time because of the relatively low cost of the constituents and their ability to produce a high deformation without breakage during drawing strain at room temperature [5–9]. Previously, it has been shown that formation of the metastable supersaturated α-(Fe, Cu) solid solution occurring during milling process makes an influence on magnetic properties and tensile strength of the Fe–Cu nanocomposites [9].

Equiatomic YCu compound belongs to the family of fully ordered and completely stoichiometric RM intermetallics (R—rare earth metal, M—transition metal) and is even more interesting from the point of view of its mechanical properties, namely, due to its unusual high ductility [10, 11]. Although YCu intermetallic is traditionally produced by arc or induction melting, we were able to synthesize this compound in its fine-grained form by mechanical alloying route [12].

In the present work, the Fe–Cu and Y–Cu nanocomposites were synthesized by mechanical alloying and the crystal structure refinement has studied. The mechanical characteristics of obtained materials were estimated.

2. EXPERIMENTAL DETAILS

Elemental Fe, Cu powders (99.6% purity, particle sizes of $\cong 100$ μm) as well as the crushed particles of yttrium (99.8 wt.%, $\cong 150$ μm) were mixed to give the desired average composition. Mixtures obtained were sealed in a vial under an argon atmosphere and placed in a high-energy planetary ball mill. Hardened stainless steel balls (15 units of 15 mm diameter) and vial (70 mm height, 50 mm diameter) with a ball-to-powder weight ratio of 20:1 were used. The vial temperature was held below 375 K during the experiments by air-cooling. The milling process was cyclic with 15 min of treatment and 30 min of cooling time. The rotation speed was equal to 1480 rpm; the acceleration was about 50 g: the pressure for a substance particle reached 5 GPa.

The full complex of the X-ray diffraction methods (XRD) has been used for testing of the samples prepared. XRD data was collected either with DRON-4 automatic diffractometer (radiation CoK_α, Fe–Cu materials) or with DRON-3M one (radiation CuK_α, Y–Cu materials). The diffraction patterns have been obtained in a discrete mode under the following scanning parameters: observation range $2\theta = 20–130°$,

step scan of 0.05°, and counting time per step at 3 s.

The original software package, developed by us for the automated DRON equipment and including full complex of standard Rietveld refinement procedure, has been used for analysis and interpretation of the X-ray diffraction data obtained [12]. This package is intended for solving different XRD tasks, namely: determination of both peak positions and integral intensities of the Bragg reflections by means of full profile analysis; carrying out qualitative and quantitative phase analysis using PDF data for phase identification and the least square method for lattice parameters refinement; testing of the structure models and refining crystal structure parameters (including coordinates, atomic position filling, texture, *etc.*).

A set of mechanical characteristics measurements has been carried out using a method of continuous indentation (the standard Berkovich diamond pyramid) at different load with registration of an indentation diagram (dependence of the load on the depths of the pyramid's penetration) by the Micron-Gamma equipment. In this case, we found the Meyer hardness, which is the average contact pressure on the indenter–sample contact surface and correlates well with the flow stress. A load varies from 0 to 100 *g* under the simple 'loading–unloading' scheme. For each state, we processed no less than 15 penetrations with 100 μm step on a surface of the samples. The indentation performed gives us a possibility to calculate the Young's modulus E of material studied.

3. RESULTS AND DISCUSSION

3.1. Phase Composition and Crystal Structure

3.1.1. Fe–Cu Nanocomposite

Elemental Fe and Cu powders were mixed with (4:1) of weight content. The charge prepared has been treated in a planetary ball mill for 120 min since previously [9] it has been shown that this specific parameters of mechanical alloying of the iron and copper powders is optimal for formation of the α-(Fe, Cu) supersaturated solid solution.

So, powder material selected after 120 min of treatment in a ball mill was thoroughly studied by XRD method. First, X-rays phase analysis has revealed that this sample is really a single-phase one containing the α-(Fe, Cu) phase with lattice parameter $a = 0.28748(4)$ nm higher than that for pure iron ($a = 0.2866$ nm). Crystal structure refinement carried out in the frame of the α-Fe type structure has shown a completely statistical distribution of the Fe and Cu atoms in 1a position of the $Im3m$ space group (Table 1). Therefore, as a result of milling process, the supersaturated α-(Fe, Cu) solid solution containing 20 at.% Cu has been synthesized.

TABLE 1. Rietveld X-ray powder diffraction data for crystal structures of the α-Fe-type structure phases formed in the Fe–Cu composites studied.

Atom	Site	Fe–Cu powder, 120 min milled				Fe–Cu compacted after milling			
		Site occ.	x	y	z	Site occ.	x	y	z
0.8Fe + 0.2Cu	1a	1.00(1)	0	0	0	1.00(1)	0	0	0
Phase composition, wt.%		α-(Fe, Cu) (100)				α-Fe(78) + Cu(22)			
Space group		$Im3m$, No. 229				$Im3m$, No. 229			
Lattice parameter a, nm		0.28748(4)				0.28674(2)			
Total isotropic B factor, nm^2		$0.43(4)\cdot10^{-2}$				$0.77(9)\cdot10^{-2}$			
Calculated copper content, at.%		20.5(3)				0			
Reliability factor		0.033				0.021			
Average grain size D, nm		27(4)				98(6)			
Crystal lattice microdeformations ε		0.00278(9)				0.00106(9)			

It should be noted that all XRD patterns of the samples obtained by mechanical alloying usually display the broadening of their diffraction peaks. Therefore, using the classical Williamson–Hall plot [13], it would be possible to estimate the average grain sizes and strains of the phases studied. For this purpose, the dependences of scaled broadening of reflections $b^*(2\theta)$ on scattering vector **S** were analysed for supersaturated α-(Fe, Cu) solid solution and other phases synthesized. The scaled broadening for each (hkl) reflection could be expressed as $b^*(2\theta) = \beta(2\theta)\cos\theta/\lambda$, where θ is the Bragg reflection, λ is the X-ray wavelength, and $\beta(2\theta)$ is the physical broadening.

For each peak of XRD pattern, the physical broadening has calculated as $\beta(2\theta) = (FWHM^2_{\exp} - FWHM^2_R)^{1/2}$ from both experimental broadening ($FWHM_{\exp}$) and instrumental function ($FWHM_R$). The scattering vector has defined as $S = 2\sin\theta/\lambda$.

Williamson–Hall plots for the main phases formed in the sample are presented at Fig. 1. Using these plots, the average grain size D could be found by extrapolating the $b^*(2\theta)$ dependences onto the $S = 0$ axes as $D = 1/b^*(2\theta)$ and average ε values, which characterize the microdeformation of crystal lattice, could be found from a slope of $b^*(2\theta)$ straight line versus S as $b^*(2\theta)/(2S)$.

Thus, the average values of both D and ε of the crystal lattice have been determined for the α-(Fe, Cu) solid solution formed in the milling product (Table 1, Fig. 1). So, one can conclude that the nanocrystalline material (the grain size is less than 30 nm) has synthesized by the mechanochemical route.

The next step in the experiment was the consolidation of a sample

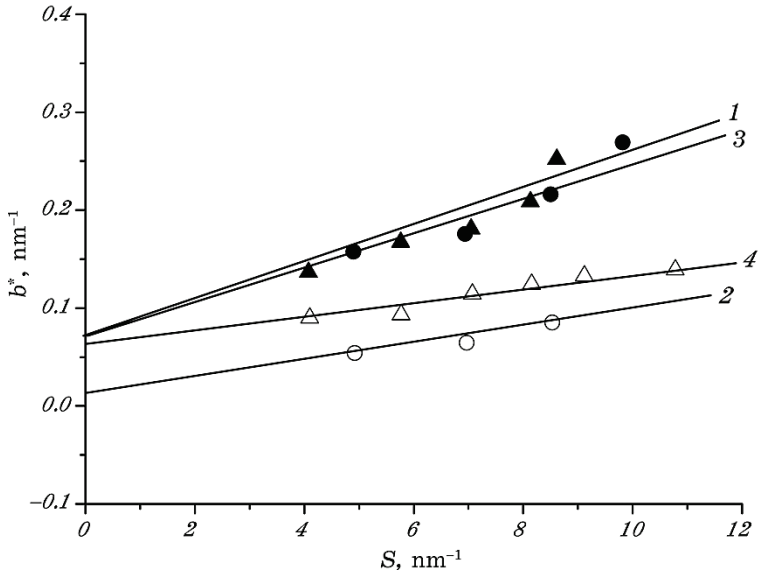

Fig. 1. Williamson–Hall plots for the phases formed in 120 min milled powder samples (*1*—α-(Fe, Cu) and *3*—YCu) as well as for phases of the compacted samples (*2*—α-Fe and *4*—YCu).

and its cold rolling. According to XRD study, the sample rolled contains two phases, namely, the pure iron and copper that has been extracted from supersaturated α-(Fe, Cu) solid solution during rolling process (Table 1). It should be noted that consolidation taking place at the rolling of powder milled is accompanied by the iron grains coarsening (up to 100 nm, Table 1) and their strongly texture in the [002] direction.

3.1.2. Y–Cu Nanocomposite

Previously [12], we have successfully synthesized the equiatomic YCu compound after 120 min of milling a charge containing elemental yttrium and copper in a planetary ball mill in air. Here, this experiment has been carried out in argon atmosphere.

According to XRD method, the powder material selected after 120 min of treatment in a ball mill in argon is two-phased and contains both YCu phase with lattice parameter ($a = 0.3473(3)$ nm) and YCu_2 intermetallic compound in approximately equal amounts. Crystal structure refinement has confirmed the fully ordered CsCl-type structure (superstructure based on the α-Fe-type lattice) for YCu compound (Table 2).

The milled sample has been consolidated by the cold pressing (applied load was equal to 6.4 GPa). According to the XRD data, the com-

TABLE 2. Rietveld X-ray powder diffraction data for crystal structure of the YCu compound (CsCl-type structure) formed after 120 min of milling.

Atom	Site	Y–Cu powder, 120 min milled				Y–Cu, compacted after milling			
		Site occ.	x	y	z	Site occ.	x	y	z
Y	1a	1.00(1)	0	0	0	1.00(1)	0	0	0
Cu	1b	1.00(1)	0.5	0.5	0.5	1.00(1)	0.5	0.5	0.5
Phase composition, wt.%		YCu(58) + YCu_2(42)				YCu(55) + YCu_2(39) + Y_2O_3(6)			
Space group		$Pm3m$, No. 221				$Pm3m$, No. 221			
Lattice parameter a, nm		0.3473(3)				0.3476(1)			
Total isotropic B factor, nm^2		$2.75(2)\cdot10^{-2}$				$0.77(9)\cdot10^{-2}$			
Calculated copper content, at.%		50.1(2)				50.2(3)			
Reliability factor		0.069				0.075			
Average grain size D, nm		26(2)				19(2)			
Crystal lattice microdeformations ε		0.00279(8)				0.00104(7)			

pact sample prepared contains YCu and YCu_2 phases as well as some amount of crystalline Y_2O_3 oxide (Table 2). Using Williamson–Hall plots (Fig. 1), the average values of D and ε of the crystal lattice have been determined for YCu compound existing either in the milling product or in the sample compacted (Table 2). Note that the material obtained in this experiment is nanostructured with a grain size less than 30 nm. Moreover, the grains of the YCu phase do not coarsen after cold pressing (Table 2).

It should be noted that existence of Cu-rich phase (YCu_2, Table 2) alongside with YCu phase is caused by the presence of oxygen in a reaction zone of a ball mill (even inside the argon atmosphere). So, the formation of the Y_2O_3 oxide shifts phase composition of the material into Cu-rich side.

3.2. Nanoindentation Measurements

As it was mentioned, the milled test samples has been consolidated by

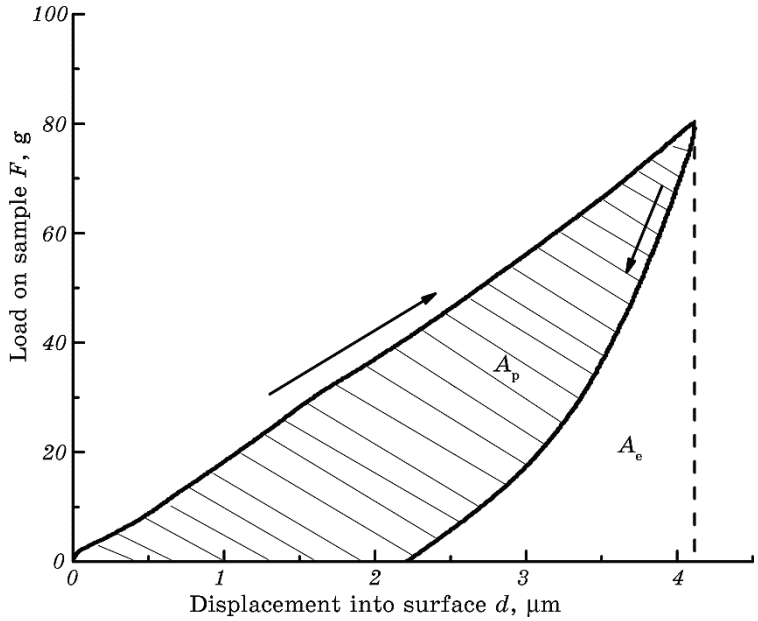

Fig. 2. Typical load–unload curve for samples studied. The areas A_p and A_e are used in calculating the plasticity parameter δ_A.

the cold pressing (applied load was equal to 6.4 GPa) for further research, in particular, to perform microhardness measurements. Figure 2 shows typical load–displacement data, which can serve to define experimental quantities based on the most widely used Oliver and Pharr analysis [14]. The entire load–unload curves exhibit similar features; the maximum load was chosen 100 g for each measurement.

The hardness evaluated from the load–displacement data reaches the value of 2.5(4) GPa (for Fe–Cu nanocomposite) and 2.7(4) GPa (for Y–Cu nanocomposite). Mechanical characteristics of nanocomposites studied (hardness, the Young's modulus, and plasticity parameter) are listed in Table 3. It should be emphasized that hardness value obtained here for YCu nanocomposite is higher than that for conventional bulk YCu intermetallic obtained by arc melting [11]. More specifically, H is

TABLE 3. Mechanical characteristics of Fe–Cu and Y–Cu nanocomposites obtained.

Nanocomposite	Fe–Cu	Y–Cu
Hardness H, GPa	2.5(4)	2.7(4)
Young's modulus E, GPa	150(5)	120(5)
Plasticity parameter δ_A	0.87	0.72

equal to 2.13(21) GPa for bulk single-phase YCu [11]. Such impressive result is due to the grain's refinement during milling process.

Plasticity parameter δ_A was determined according to [15–17] and calculated from the ratio of the areas in a continuous indentation diagram as the fraction of work A_p (Fig. 2) of plastic deformation in total indentation work A_t (Fig. 2, *a*) by the relationship:

$$\delta_A = \frac{A_p}{A_t} = 1 - \frac{A_e}{A_t},$$

where A_e and A_t are the areas under the unloading and loading curves, respectively, and $A_p = A_t - A_e$. Plasticity parameter δ_A found by continuous impression during nanoindentation is an analogue of dimensionless plasticity parameter δ_H (*i.e.*, the fraction of plastic deformation in the total elastoplastic deformation under an indenter), which characterizes the formability of a material during deformation that is retained after unloading and determined during static tests [16]. Numerous theoretical and experimental studies [18–20] show that $\delta_A \approx \delta_H$ at a sufficient accuracy. In our experiment, the plasticity characteristic δ_A is equal to 0.87 for Fe–Cu and reaches 0.72 for Y–Cu nanocomposite.

It is interesting to note that the Young's modulus E of Fe–Cu nanocomposite obtained is smaller than that of bulk FeCu alloy. Namely, E is equal to 150(5) GPa for Fe–Cu nanocomposite while E for bulk FeCu reaches to 210(10) GPa. [15]. According to the data obtained, this decrease is approximately 30%. In a case of Y–Cu nanocomposite, E reaches 120(5) GPa. Unfortunately, to our knowledge, there is no experimental data regarding the Young's modulus available for YCu compound, but a number of theoretical calculations have been made [21–23]. However, E value obtained here is lower than theoretically predicted one (133 GPa) [21–23].

According to the composite model of Mughrabi [19, 20], the decrease in E values can occur as a result of an increase in the volume fraction of the intergranular space—the grain boundaries and triple junctions, the mechanical properties for which differ from the properties of the grain body. In addition, the reduction in the grain size leads to an increase in the part of free volume within the grain boundaries, in the boundary areas and in triple junctions. This causes the weakening of atomic bonds in a nanostructured material.

4. CONCLUSIONS

Fe–Cu and Y–Cu mechanically alloyed nanocomposites have been synthesized in a high-energy planetary ball mill from elemental powders of Fe, Cu and crushed particles of Y. As a result of milling process, the supersaturated α-(Fe, Cu) solid solution containing 20 at.% Cu with

the fully disordered α-Fe-type structure and YCu compound with fully ordered CsCl-type structure (superstructure based on the α-Fe-type lattice) have been obtained.

The mechanical characteristics of obtained Fe–Cu and Y–Cu nanocomposites have been analysed. It should be emphasized that hardness for both Fe–Cu and Y–Cu obtained here materials is higher than that for conventional bulk alloys. Such impressive result is due to the grains' refinement during milling process mainly. However, the Young's modulus E of obtained FeCu nanocomposite is smaller than that of bulk FeCu alloy. According to the obtained data, this decrease is approximately 30%.

REFERENCES

1. C. Suryanarayana and N. Al-Aqeeli, *Progr. Mater. Sci.*, **58**, Iss. 4: 383 (2013).
2. C. Suryanarayana, *Progr. Mater. Sci.*, **46**, Iss. 1–2: 1 (2001).
3. E. Ma, *Prog. Mater. Sci.*, **50**, Iss. 4: 413 (2005).
4. P. H. Shingu and K. N. Ishihara, *Mater. Trans.*, **36**, Iss. 2: 96 (1995).
5. R. B. Schwarz and C. C. Koch, *Appl. Phys. Lett.*, **49**, Iss. 3: 146 (1986).
6. J. Eckert, L. Schultz, and K. Urban, *Appl. Phys. Lett.*, **55**, Iss. 2: 117 (1989).
7. E. Hellstern, H. I. Fecht, Y. Fu, and W. L. Johnson, *J. Appl. Physics*, **65**: 305 (1989).
8. V. L. Tagarielli, N. A. Fleck, A. Colella, and P. Matteazzi, *J. Mater. Sci.*, **46**, Iss. 2: 385 (2011).
9. O. Boshko, O. Nakonechna, M. Dashevskyi, K. Ivanenko, N. Belyavina, and S. Revo, *Adv. Powder Technology*, **27**, Iss. 4: 1101 (2016).
10. K. Gschneidner Jr., A. Russell, A. Pecharsky, J. Morris, Z. Zhang, T. Lograsso, D. Hsu, C. H. C. Lo, Y. Ye, A. Slager, and D. Kesse, *Nature Materials*, **2**, No. 9: 587 (2003).
11. A. M. Russell, Z. Zhang, K. A. Gschneidner Jr., T. A. Lograsso, A. O. Pecharsky, A. J. Slager, and D. C. Kesse, *Intermetallics*, **13**, Iss. 6: 565 (2005).
12. M. Dashevskyi, O. Boshko, O. Nakonechna, and N. Belyavina, *Metallofiz. Noveishie Tekhnol.*, **39**, No. 4: 541 (2017).
13. H. P. Klug and L. E. Alexander, *X-Ray Diffraction Procedures for Polycrystalline and Amorphous Materials* (New York: Wiley: 1974).
14. W. C. Oliver and G. M. Pharr, *J. Mater. Res.*, **7**, Iss. 6: 1564 (1992).
15. I. N. Frantsevich, F. F. Voronov, and S. A. Bakuta, *Elastic Constants and Elastic Moduli of Metals and Nonmetals: A Handbook* (Kiev: Naukova Dumka: 1982) (in Russian).
16. Yu. Milman, S. Dub, and A. Golubenko, *Symposium AA—Fundamentals of Nanoindentation and Nanotribology IV*, **1049**: 1049-AA05-06 (2007).
17. D. Tabor, *The Hardness of Metals* (Oxford: Clarendon Press: 2000).
18. V. A. Pozdnyakov and A. M. Glezer, *Phys. Solid State*, **44**, Iss. 4: 732 (2002).

19. T. Ungar, H. Mughrabi, D. Rönnpagel, and M. Wilkens, *Acta Metall.*, **32**, Iss. 3: 333 (1984).
20. H. Mughrabi, *Acta Metall.*, **31**, Iss. 9: 1367 (1983).
21. A. Sekkal, A. Benzair, H. Aourag, H.I. Faraoun, and G. Merad, *Physica B*, **405**, Iss. 13: 2831 (2010).
22. J. R. Morris, Y. Ye, Y. B. Lee, B. N. Harmon, K. A. Gschneidner Jr., and A. M. Russell, *Acta Mater.*, **52**, Iss. 16: 4849 (2004).
23. S. S. Chouhan, P. Soni, G. Pagare, S. P. Sanyal, and M. Rajagopalan, *Physica B*, **406**, Iss. 3: 339 (2011).